2 **The Climate Impact of Aerosols on Lightning: Is it Detectable from**

3 **Long-term Aerosol and Meteorological Data?**

8 Qianqian Wang[1], Zhanqing Li*[1,2], Jianping Guo*[3], Chuanfeng Zhao[1], Maureen Cribb[2]
9
10
11
12
13
14 [1]State Laboratory of Earth Surface Process and Resource Ecology, College of Global Change and
15 Earth System Science, Beijing Normal University, Beijing, China.
16 [2]Earth System Science Interdisciplinary Center, University of Maryland, College Park, MD,
17 USA.
18 [3]State Key Laboratory of Severe Weather, Chinese Academy of Meteorological Sciences,
19 Beijing, China

28 **March 9, 2018**

Abstract

32   Aerosol effect on lightning is still under debate. In this study, the relative roles of meteorology

33   and aerosols on lightning activities in Africa are investigated from a climatological perspective,

34   based on the 11-year worth of lightning flashes from Lightning Imaging Sensor onboard Tropical

35   Rainfall Measuring Mission, aerosol optical depth (AOD) from Moderate Resolution Imaging

36   Spectroradiometer onboard Aqua, meteorological variables from the Medium-Range Weather

37   Forecasting ERA-Interim reanalysis and aerosol composition data from the Modern-Era

38   Retrospective analysis for Research and Application. Six meteorological variables are selected:

39   sea level pressure (SLP), potential temperature (θ) at 2 m above ground level, mid-level relative

40   humidity (RH), convective availabe potential energy (CAPE), vertical wind shear (SHEAR), and

41   200 hPa divergence (Div). To differentiate two dominant aerosol types in Africa and to account for

42   their distinct climate regimes that all affect lightning, we separate two regions of interest (ROIs):

43   the northern Africa (ROI_1) and the southern Africa (ROI_2) dominated by dust and smoke

44   aerosols, respectively. As compared with dust in ROI_1, smoke aerosols in ROI_2 exhibit huge

45   contrast between dry and wet season. Irrespective of regions, the lightning exhibits large diurnal

46   variation with an afternoon peak and strong seasonality with a summertime peak, while the

47   pronounced differences in lightning under relatively clean and polluted conditions signify the

48   potential influences of aerosols. Lightning is dictated mostly by RH and CAPE in the dust

49   dominant region (ROI_1). In the smoke dominant region (ROI_2), the effect of SLP is also

50   significant. Systematic changes of boomerang shape are found in lightning frequency with AOD,

51   with a turning point at around AOD=0.3, below which lightning flashes increase monotonously

52   with increasing AOD in both ROIs. As AOD approaches the optimal value, lightning activity seems

53   to be saturated under smoky condition, likely due to the tradeoff between the aerosol invigoration

54   effect and the radiative effect that tends to enhance and suppress lightning, respectively. In contrast,

55   lightning activity in ROI_1 is suppressed by dust aerosol presumably due to the more dominant

56   radiative heating effect of dust aerosol under dry environment.

1.Introduction

Lightning can be considered as a key indicator of strong atmospheric convection [*Betz et al.*, 2008], generally accompanied with a concomitant severe storms. Lightning activities have been linked with two major factors: meteorology and aerosols (e.g. Bell et al., 2009; Bell et al., 2008; Boccippio et al., 2000; Christian et al., 2003; Farias et al., 2014; Guo et al., 2016; Lucas et al., 1994; Orville et al., 2001; Williams and Stanfill, 2002; Williams et al., 2004; Williams et al., 2005).

Since the pioneering work in 1990's by Westcott (1995) who attempted to link the summertime cloud-to-ground lightning activity to anthropogenic activities, the roles of aerosols in lightning have been increasingly recognized, as comprehensively reviewed on the topic associated with aerosol-cloud-precipitation interactions (e.g. Tao et al., 2012, Fan et al., 2016; Li et al., 2016; 2017a). The aerosol effect can be generally divided into radiative and microphysical effects (Boucher et al., 2013; Li et al., 2017b). The radiative effect suggests aerosols can heat the atmospheric layer and cool the surface by absorbing and scattering solar radiation, thereby reducing the latent heat flux and stabilizing the atmosphere (Kaufman et al., 2002; Koren et al., 2004; Koren et al., 2008; Li et al., 2017a). As a consequence, convection and electrical activities are likely inhibited (Koren et al., 2004). By acting as cloud condensation nuclei (CCN) with the constrained water, increasing aerosols loading tends to reduce the mean size of cloud droplets, suppress coalescence and delay the onset of warm-rain processes (Rosenfeld and Lensky, 1998), which permits more liquid water to ascend higher into mixed phased region where it fuels lightning. A conspicuous enhancement of lightning activity was found to be tightly connected to volcanic

77   ashes over the western Pacific Ocean (Yuan et al., 2011) and aerosol emissions from ships over the

78   equatorial Indian Ocean (Thornton et al., 2017). In terms of the response of clouds to aerosols, an

79   optimal aerosol concentration was found to exist, based on observation analysis (Koren et al., 2008;

80   Wang et al., 2015) and a simple parcel model calculation (Rosenfeld et al., 2008). Biomass burning

81   activities, anthropogenic emission and desert dust are the three major atmospheric aerosol sources

82   (Rosenfeld et al., 2001; Li et al. 2011; Fan et al. 2018), which are recognized to have different

83   climate effects. The increased rainfall in the south China and drought in the north China are thought

84   to be related with increased black carbon aerosols (Menon et al., 2002) while the effect of dust on

85   cloud properties tends to decrease precipitation from a feedback loop (Rosenfeld et al., 2001).

86   However, most studies on aerosol-convection interactions account for aerosol burden (i.e.

87   AOD, the number concentration of aerosol, $PM_{2.5}$, or CCN) rather than aerosol species. It was not

88   until recently that the effect of aerosol species in modulating lightning activities was investigated

89   (e.g. Stolz et al., 2015; 2017), which prompts us to perform more detailed analyses in this study.

90   The lightning and convection strength are controlled by various meteorological variables and

91   indices such as air temperature (T) (Price, 1993; Williams, 1994; 1999), the convective available

92   potential energy (CAPE) and its vertical distribution (normalize CAPE, NCAPE) (Bang and Zipser,

93   2016; Stolz et al., 2015), vertical wind shear (SHEAR) (Fan et al., 2009; 2013; Igel and Heever,

94   2015; Khain et al., 2008), relative humidity (RH) in the lower and middle troposphere (Fan et al.,

95   2007; Wall et al., 2014), cloud base height (Williams et al., 2005), updraft velocity (Williams et

96   al., 2005; Zipser and Lutz, 1994), and warm cloud depth (Stolz et al., 2015, 2017).

97   Depending on aerosol properties and atmospheric conditions, aerosols may enhance (Fan et al.,

2007; Khain et al., 2005; 2008) or suppress convection (Khain et al., 2004; Rosenfeld, 2000;

Rosenfeld et al., 2001; Zhao et al., 2006). In general, aerosols tend to suppress convection for

isolated clouds formed in relatively dry condition but to invigorate convection for convective

systems inside a moist environment. Under conditions of strong vertical wind shear, aerosols tend

to reduce the strength of single deep convection clouds due to higher detrainment and larger

evaporation of cloud hydrometeors (Richardson et al., 2007; Fan et al., 2009), thereby altering the

lightning activities (Altaratz et al., 2010; Farias et al., 2014). Apart from invigoration effect

induced by aerosol, lightning activities are enhanced by increases in NCAPE and SHEAR, but

inhibited by increasing RH and warm cloud depth (Stolz et al., 2015).

Most previous studies were based on short-term data, while we try to employ long-term (11

years) lightning and meteorological data to investigate and quantify the relative roles of aerosol

and meteorology on lightning. Section 2 describes the dataset and method used in this study,

Section 3 shows regions of interest, and Section 4 examines (1) long-term climatological features

of lightning and aerosol, (2) differences of lightning, AOD, meteorological variables under

relatively clean and polluted conditions, (3) response of lightning to meteorology, (4) contrast in

the response of lighting to dust and smoke aerosol, and (5) relative roles of meteorology and AOD

in lightning activity, finally followed by a summary of the key findings in section 5.

2. Data and Method

2.1 Data

2.1.1 Lightning data

118   We employ lightning data from the Lightning Imaging Sensor (LIS) onboard Tropical Rainfall

119   Measuring Mission (TRMM), which is designed to acquire and investigate the distribution and

120   variability of total lightning (i.e. intra-cloud and cloud-to-ground) on a global basis, span all

121   longitudes between 38°N-38°S, during day and night (Boccippio, 2002; Christian et al., 2003).

122   The LIS on TRMM monitors individual storms and storm systems at a nadir field of view

123   exceeding 580 km×580 km with a detection efficiency of 69%-90%. We employ the gridded

124   lightning climatology dataset during a 11-year period (2003-2013) called the low resolution

125   monthly time series (LRMTS) that provides flash rate per month at a 2.5°×2.5° spatial resolution

126   and is recorded in coordinated universal time (UTC). The low-resolution diurnal climatology

127   (LRDC) depicts the mean diurnal cycle in local solar time (LT) on the same spatial resolution

128   (Cecil et al., 2001; 2006; 2014).

129   *2.1.2 Aerosol data*

130   Aerosol loading is characterized by aerosol optical depth (AOD), which is obtained from

131   observations collected by the Moderate Resolution Imaging Spectroradiometer (MODIS) onboard

132   Aqua satellite that passes at ~ 13:30 local time (LT). Here, the level 3 atmosphere monthly global

133   product (MYD08_M3) on 1°×1° grid is used. This AOD is retrieved at 0.55 μm, based on dark

134   target-deep blue combined algorithm, which is particular suitable over desert regions (Hubanks et

135   al., 2015; Levy et al., 2013). The Modern Era Retrospective-analysis for Research and Application

136   (MERRA) is a NASA meteorological reanalysis taking advantage of satellite data dated to 1979

137   till present using the Goddard Earth Observing System Data Assimilation System Version 5

138 (GEOS-5). The assimilation of AOD in the GEOS-5 involves very careful cloud screening and

139 data homogenization by means of a Neural Net scheme that translates MODIS radiances into

140 Aerosol Robotic Network (AERONET) calibrated AOD. The MERRA Aerosol Re-analysis

141 (MERRAero) provides dust, black carbon, organic carbon, and total extinction AOD, and the total

142 Angstrom Exponent (AE) at a spatial resolution of 0.625°×0.5° (da Silva, et al., 2015). These data

143 characterize aerosol species and particle size.

144 *2.1.3 Meteorological data*

145 Meteorological data utilized are from the Medium-Range Weather Forecasting (ECMWF)

146 ERA-Interim reanalysis product (Dee et al., 2011), including the surface upward sensible heat flux

147 (SHF), surface upward latent heat flux (LHF), sea level pressure (SLP), 2m air temperature (T),

148 convective available potential energy (CAPE), relative humidity (RH), wind field at 925 hPa and

149 500 hPa (U, V), divergence at 200 hPa (Div) with a spatial resolution of 1°×1°. With reference to

150 the findings from previous studies, we choose the following factors to characterize meteorology:

151 1) Convective available potential energy (CAPE). CAPE is the most commonly used

152 thermodynamic parameter, which describes the potential buoyancy available to idealized rising

153 air parcels and thus denotes the instability of atmosphere (Riemann-Campe et al., 2009;

154 Williams, 1992). The bigger it is, the atmosphere is more unstable, and more favorable to the

155 occurrence and development of convection. Lightning activity increases with the CAPE

156 (Williams, 1992). The conversion efficiency of CAPE to updraft kinetic energy (Williams et

157 al., 2005) depends on the strength and width of updraft. Unfortunately, we don't have any

158   reliable updraft measurements to tackle with its role in this study.

159   2) Sea level pressure (SLP). It's widely known that pressure is a key meteorological factor

160   affecting the weather, for it defines basic weather regimes. Low pressure systems are usually

161   associated with strong winds, warm air, and atmospheric lifting, thus normally producing

162   clouds, precipitation, and severe weather events such as storms and cyclones. The implication

163   of summertime SLP anomalies in the tropical Atlantic region shows the inverse relationship

164   between SLP and tropical cyclones (Knaff, 1997).

165   3) Potential temperature (θ). Many researchers have studied the role of air temperature in

166   influencing lightning activities (Markson, 2003; Williams, 1992; 1994; 1999; Williams et al.,

167   2005). However, the direct comparison of temperature for different regions is problematic

168   because air temperature is systematic decline with altitude. We choose potential temperature

169   instead, which corrects for the altitude dependence and provides a more meaningful

170   comparison. Here, potential temperature θ is calculated from 2 m air temperature T (K):

171    $$\theta = \mathrm{T}(\frac{1000}{p})^{0.286} \qquad\qquad (1)$$

172   4) Relative humidity (RH). As one of the important thermodynamic factors, RH has been

173   identified to affect the relationship between aerosols and convection (Fan et al., 2007; Fan et

174   al., 2009; Khain and Lynn, 2009). It was found that for isolated clouds formed in a relative dry

175   condition convection is suppressed by aerosols, whereas for convective systems inside a moist

176   environment convection is invigorated (Khain and Lynn, 2009; Khain et al., 2008). The mean

177   RH values at 700 and 500 hPa levels (mid-level RH) are employed in this study.

178   5) Wind Shear. The vertical shear of horizontal wind (U, V), hereafter simply referred as wind

179   shear or SHEAR, has been shown not only to affect the dynamical flow structures around and

180   within a deep convective cloud (Coniglio et al., 2006; Rotunno et al., 1988; Weisman and

181   Rotunno, 2004), but also qualitatively determines whether aerosols suppress or enhance

182   convective strength (Fan et al., 2009). It is calculated from daily wind field at 925hPa and

183   500hPa as follows:

184    $$\text{SHEAR} = \sqrt{(U_{500} - U_{925})^2 + (V_{500} - V_{925})^2} \qquad (2)$$

185   6) Divergence (Div). Air divergence is especially useful, because it can be linked to diabatic

186   heating processes, of which, the non-uniformity gives rise to atmospheric motion (Homeyer et

187   al., 2014;Mapes and Houze, 1995). Fully developed clouds are usually accompanied by upper-

188   level divergence especially in raining regions (Mapes and Houze, 1993). A pronounced

189   divergence maximum exists between 300 and 150 hPa due to deep convective outflow

190   (Mitovski et al., 2010).

191   Besides, bowen ratio (BR) is calculated from SHF and LHF to describe surface property:

192    $$\text{BR} = \frac{SHF}{LHF} \qquad (3)$$

193   *2.2 Method*

194   *2.2.1 Data collocation*

195   A roughly three-month smooth average is chosen to allow LIS to progress through the diurnal

196   cycle at a given location twice (Cecil et al., 2014), and show the normal annual variation of

197   lightning activity due to the seasonal meridional migration of the intertropical convergence zone

198   (Thornton et al., 2017; Waliser and Gautier, 1993). In order to match lightning data, all AOD and

199   meteorological data are calculated by taking 3-month running mean and resampled to 2.5°×2.5°

200   resolution grids in the climatic analysis. In order to make the comparison within the same AOD

201   range and increase the number of data samples, climatological features of lightning, AOD and

202   meteorology under polluted and clean conditions are limited to the cases with AOD<1.0 over both

203   ROIs. The top third of AOD is labeled as polluted case and the bottom lowest third is labeled as

204   clean case. All data are sorted by AOD, and divided into three equal-sample subsets to create

205   sufficient contrast between polluted and clean conditions.

206   *2.2.2 Statistical analysis method*

207   Correlation coefficients are used in statistics to measure how strong a relationship between

208   lightning flashes and one predictor (SLP, θ, RH, CAPE, SHEAR, Div, AOD). Pearson correlation

209   is commonly used in measuring linear correlation. And partial correlation is performed to control

210   other predictors and make it possible to study the effect of each predictor separately. The

211   correlation is considered to be significant when it passes the significant test at 0.05 level.

212   In order to explore the relative roles of meteorological variables and AOD in lightning

213   activities, we use multiple-linear regression method follow previous studies (e.g. Igel and van den

214   Heever, 2015; Stolz et al., 2017) and establish standardized regression equation for AOD greater

215   and less than 0.3 respectively. This subsection regression is performed to reduce nonlinear effect

216   of AOD. Note that, all data used here are processed by averaging 10 samples sorted by AOD from

217   small to large to mitigate data uncertainties. The standardized regression equation with seven

218   predictor variables x_1, x_2,…, x_7 (SLP, θ, RH, CAPE, SHEAR, Div, AOD) and a response y

219   (lightnng flashes), can be written as:

220 $$y = \beta_0 + \beta_1 x_1 + \beta_2 x_2 + \cdots + \beta_i x_i, \qquad i = 1, \dots ,7 \qquad\qquad (4)$$

221   Here, y and x_i are standardized variables, which are derived from raw variables Y and X_i by

222   subtracting the sample mean $(\overline{Y}, \ \overline{X_I})$ and divided by the sample standard deviation $(\delta_Y, \ \delta_i)$:

223 $$y = \frac{Y - \overline{Y}}{\delta_Y}, \qquad x_i = \frac{X_i - \overline{X_I}}{\delta_i}, \qquad\qquad i=1, \dots ,7 \qquad\qquad (5)$$

224   The sample mean is calculated of N valid samples:

225 $$\overline{Y} = \frac{\sum_1^N Y_j}{N}, \qquad \overline{X_I} = \frac{\sum_1^N X_{ji}}{N}, \qquad i=1, \dots ,7; \quad j=1, \dots ,N \qquad\qquad (6)$$

226   The sample standard deviation is:

227 $$\delta_Y = \sqrt{\frac{1}{N-1} \sum_1^N (Y_j - \overline{Y})^2}, \qquad \delta_i = \sqrt{\frac{1}{N-1} \sum_1^N (X_{ji} - \overline{X_I})^2}, \qquad i = 1, \dots ,7; \quad j = 1, \dots ,N \qquad (7)$$

228   Standardized regression coefficients ignore the independent variables' scale of units, which make

229   slop estimate comparable and show the relative weights to the changes of lightning flashes.

230   **3. Region of Interest (ROI)**

231   The northern and southern Africa has high aerosol loadings of dust and smoke aerosols

232   respectively, as seen in Fig. 1. Northern Africa is the world's largest source of mineral dust

233   (Lemaître et al., 2010), with the most widespread, persistent dust aerosol plumes and the most

234   dense particulate contribution found on Earth (Prospero et al., 2002). It has been estimated about

235   2-4 billion tons of blown dust globally comes from the Saharan desert (Goudie and Middleton,

236   2001). Dust of relevance to atmospheric processes are the minerals that can be readily suspended

237   by wind (Shao, 2008) with particle size up to 70 μm. Besides, Africa is also the single largest

238   source of smoke emissions due to widespread biomass burning, accounting roughly for 30 to 50%

239   of the total amount of vegetation burned globally each year (Andreae, 1991; Roberts et al., 2009;

240   van der Werf et al., 2003; 2006). In Central and Southern Africa, biomass burning due to wildfires

241   and human-set fires has strong diurnal and seasonal variability (Ichoku et al., 2016; Roberts et al.,

242   2009).

243   The upper left panel of Figure 1 shows the global distribution of mean aerosol optical depth

244   (AOD) from the MODIS onboard Aqua satellite during the period from 2003 to 2013. The lower

245   left panel is the Angstrom Exponent (AE) obtained from the Modern-Era Retrospective analysis

246   for Research and Application (MERRA) Aerosol Reanalysis (MERRAero) at a 0.625°×0.5° spatial

247   resolution for analysis of contributions from different aerosol species, chiefly, dust, black carbon

248   (BC), organic carbon (OC) and total extinction AOD. Note that the satellite retrievals of the AE

249   have too large uncertainties over land. The Africa stands out very distinctly with very large AOD

250   in two regions: Sahara covered by dust (the upper right panel) and central to south (lower right

251   panel) Africa by smoke, characterized by small and large values of angstrom index (lower left

252   panel). Due to their distinct differences in aerosol species, they are selected as the regions of our

253   interest ROI_1 and ROI_2 (Fig. 2a). The ratios of dust (ROI_1) or (BC+OC) (ROI_2) extinction

254   AOD to total extinction AOD are larger than 50% averaged over the period 2003-2013, which

255   enables us to study any different effects on lightning activities.

256   ## 4.   Results and Discussion

257   *4.1 Long-term climatological features of lightning and aerosol*

258   Figure 2a shows the mean wind vector at 850 hPa from the ERA-Interim re-analysis at a spatial

259 resolution of 1°×1° over the Africa and the neighbouring ocean over the region defined in Fig. 1

260 (red rectangle). Figure 2 also shows the the diurnal cycle (b) and monthly variation (c, d) of AOD

261 and lightning flashes as caculated under relatively clean and polluted (dusty/smoky) conditions

262 over dust dominant region (ROI_1) and smoke aerosol dominant region (ROI_2) with color orange

263 and black, respectively. Note that AOD used hereinafter is derived from MODIS, and the lowest

264 (highest) third of AOD is labeled as clean (polluted) condition. The diurnal curves in Fig. 2b show

265 the same afternoon peak in lightning activities, which is in accordance with the strong convection

266 in terms of both the number and intensity of convective clouds in afternoon over land (Nesbitt and

267 Zipser, 2003). Over both ROI_1 and ROI_2, the lightning peak times under polluted (dusty/smoky)

268 conditions are delayed by about 1h compared with that under clean condition. This result is

269 consistent with the obsevation-based finding in southern China (Guo et al., 2016) and model

270 simulation results by Lee et al. (2016). Numerous studies have noted that aerosols modulate

271 convection and lightning activities through both radiative and microphysical processes, as

272 reviewed extensively by Li et al. (2016) in Asia and around the world (Li et al., 2017b). When we

273 look into the monthly variation, dust loading changes little through the whole year (Fig. 2c), while

274 smoke shows pronounced seasonal variation of a huge contrast between dry and wet seasons (Fig.

275 2d). Lightning in both regions is most active in summer and rarely occurs in winter, which implies

276 that lightning activity is mainly controlled by thermodynamic conditions. Besides, also shown in

277 Fig. 2 is the apparent enhancement of lightning activity under smoky conditions superimposed on

278 both the diurnal and seasonal cycles. Under dusty conditions, however, the impact is much weaker.

279 Apart from different aerosol effects, different climate conditions between dust and smoke aerosol

280   dominant region may also contribute. A key factor is relative humidity which is much lower over

281   the desert region of ROI_1 (BR>10) than over the moist region of ROI_2 covered with rain forest

282   (BR<0.4). It's widely known that high values of relative humidity are more favorable for the

283   invigoration effect and vice versa (Fan et al., 2008; 2009; Khain, 2009; Khain et al., 2008), which

284   is likely a major cause for the difference. Besides, ROI_1 locates in the vicinity of the African

285   Easterly Jet (AEJ) (Burpee, 1972) while ROI_2 locates in the ITCZ (Waliser and Gautier, 1993)

286   that lead to differences in wind shear and instability.

287   *4.2 Response of lightning to meteorology*

288   As thermodynamic condition is considered to play the main role in lightning diurnal and

289   seasonal variation. Firstly, we have a look at the response of lightning to thermodynamic condition

290   which is characterized by six meteorological variables (SLP, SHEAR, θ, CAPE, RH and Div).

291   Violin plot is an effective and attractive way to visualize the distribution of the data and the shape

292   of distribution that allows quick and insightful comparison of multiple distributions across several

293   levels of categorical variables, and is used in the analysis between lightning and meteorological

294   variables. It synergistically combines the box plot and the density trace into a single display (Hintze

295   and Nelson, 1998).

296   Figure 3 shows the linear relationships between lightning flashes and six meteorological

297   variables in ROI_1. CAPE, RH and Div are the top three meteorological variables strongly and

298   positively correlated with lightning flashes (R>0.7), which suggests that high RH and CAPE are

299   conductive to the development of intense convection and lightning occurrence that is always

300   associated high level divergence. One thing to notice is the variable density shape in Fig. 3f. The

301   bimodal distribution indicates that small to moderate high level divergence may due to atmosphere

302   movement in clear sky or in-cloud with smaller updraft velocity that doesn't produce lightning,

303   while large divergence usually characterize strong upward movement which is closely associated

304   with lightning activity. Figures 3a, e show inverse correlations of lightning flashes to SLP and

305   SHEAR and Figure 3b shows weak correlation to θ, all with quite small correlation coefficients

306   that can not be considered as correlated.

307   Figure 4 shows the linear correlations between lightning flashes and six meteorological

308   variables associated with strong convection for ROI_2. It is evident that RH, CAPE, and Div are

309   positively associated with the occurrence of lightning, in sharp contrast to SLP, θ, and SHEAR that

310   are negatively connected with lightning. In particular, Figures 4a, c, d, e show that CAPE, RH,

311   Div, and SLP are significantly correlated with lightning ($|R|>0.75$, $p<0.05$), indicating that these

312   four meteorological variables could be the major factors modulating the changes in lightning. By

313   comparison, the weak linear relationship exists between lightning and θ (R=0.47), which is case

314   for the relationship between lighting and SHEAR (R=-0.08), indicative of their minor effect on

315   lightning (Figs. 4b, 4g). Note that the correlation coefficients obtained here can only describe the

316   possible dependencies between lightning and meteorological variables, which cannot imply the

317   causal relationship.

318   In order to give a visual comparison of ROI_1 and ROI_2, we show the spatial distribution of

319   correlation coefficients between lightning and meteorological variables. Spatially, Figure 5 shows

320   that lightning flashes are well correlated with RH, CAPE, and Div throughout ROI_1 and ROI_2.

321   After we constrain the variations of AOD and other five meteorological variables, partial

322   correlation analyses show that only CAPE and RH are the top two factors affecting lightning

323   activities (Fig. 6).

324   *4.3* Contrast in the response of lighting to dust and smoke aerosol

325   Aerosols can modulate lightning activities through participating in radiative and microphysical

326   processes. The roles of dust and smoke aerosols in modulating lightning activity are examined in

327   Fig. 2 and Fig. 7. The diurnal cycle of lightning flashes in Fig. 2 shows that, for both dust and

328   smoke aerosols, the lightning peak times under polluted conditions are delayed by about 1h.

329   Besides, smoke aerosols tend to apparently enhance lightning activity on both diurnal and seasonal

330   cycles, while the impact of dust is much weaker.

331   Figure 7 shows that from clean to polluted condition, lightning response to AOD in an apparent

332   boomerang shape (Koren et al., 2008) in both dust and smoke aerosol dominant regions, with a

333   turning point around AOD=0.3. In order to reduce the effect of non-linearity, data are divided into

334   two subsets before and after the turning point when perform correlation and regression. For AOD

335   less than 0.3, lightning flashes increase monotonously with increasing aerosol loading in both

336   regions. Clusters of the data are aligned around the regression lines rather tightly, implying that

337   lightning flashes are strongly and positively correlated (R>0.75) with AOD. However, for AOD

338   exceeding 0.3, the data points are more scattered and the trend is reversed, which imply that under

339   large aerosol loadings, lightning is mainly influenced by other factors, such as meteorology.

340   Specifically, under smoky conditions, the correlation coefficient becomes negative (-0.15) and fails

341   the significant significance test at 0.01 level, suggesting a suppressing effect is yielding to the

342   invigoration effect. Under dusty conditions, the negative correlation is more significant with a

343   correlation coefficient of -0.41, suggesting a stronger suppression under heavy dust conditions

344   (Farias et al., 2014). Besides, we can easily find that lightning activity is much more intense in

345   smoke aerosol dominant region that located in ITCZ where air is hot and humid, regardless of

346   aerosol loading. In contrast, dust dominant region is much drier that is not so easy to produce

347   intense convection and lightning.

348   *4.4 Environmental dependence of aerosol effect*

349   To further clarify the joint influences of meteorology and aerosols on lightning activity, the

350   distribution of lightning flashes with AOD and the top two influential meteorological variables RH

351   and CAPE (based on the results in Figs. 3-6) are examined in Fig. 8. Lightning flashes are classified

352   into 100 discrete cells by ten decile bins of AOD – CAPE, AOD – RH, and CAPE – RH

353   respectively, which ensures approximately equal sample sizes among the cells. The mean values

354   are calculated in each cell. Results show that, for each CAPE bin, lightning flashes increase with

355   increasing aerosol loadings under relatively clean condition, but decrease after the turning point

356   around AOD=0.3 in both regions. When AOD is fixed, lightning flashes monotonically increase

357   with CAPE. Irrespective of aerosol loadings and regions, lightning rarely occurs when CAPE is

358   less than 100 J kg^{-1} from a climate perspective, that accounts for about half of the data in ROI_1.

359   Systematically higher CAPE in ROI_2 induces more intense lightning activity than in ROI_1.

360   However, lightning flashes response to RH in different ways for ROI_1 and ROI_2 when AOD is

361   fixed (Figs. 8b, 8d). In dust dominant region, lightning flashes monotonically increase as RH

362   increases under any level of aerosol loadings, but changes a little as AOD increases in each RH

363   bin. This suggests that, apart from CAPE, RH is another constraint of lightning activity in ROI_1.

364   But for smoke aerosol dominant region, high lightning flashes appear in the environment of

365   moderate RH and high aerosol loadings. When RH is fixed, the response of lightning flashes to

366   AOD also shows a turning point in AOD around AOD=0.3, beyond 0.3, lightning flashes remain

367   high value. When looking into the common role of RH and CAPE on lightning, the data distributes

368   along the diagonal which shows that RH is highly correlated with CAPE, and they affect lightning

369   activity in the same direction. Generally, intense lightning activity occurs under the condition of

370   both high RH (>40%) and high CAPE (>100 J kg^{-1}) in ROI_1. In ROI_2, high CAPE and high RH

371   are still conductive to lightning production, but data disperse in a larger range, which suggests that

372   the correlation of RH and CAPE are not as high as in ROI_1, and the restriction of RH is reduced.

373   As shown in Fig. 2 and Figs. 7, 8, the differences of lightning response to aerosols in ROI_1

374   and ROI_2 may also contribute to different climate conditions. In order to isolate the signal

375   attributed to aerosol loadings from that attributed to environmental forcing, lightning flashes are

376   separated by six meteorological variables (SLP, SHEAR, θ, CAPE, RH and Div) respectively.

377   Figure 9 shows the differences of lightning flashes between polluted and clean conditions (polluted

378   minus clean datasets) as a function of SLP, SHEAR, θ, CAPE, RH and Div. Generally, there are

379   more lightning flashes for all these meteorological variables under polluted conditions when

380   compared with that under clean conditions in both ROI_1 and ROI_2. All the lighting enhancement

381   under polluted conditions are highly significant (>99%), based on Student's test. The differences

of lightning flashes between polluted and clean conditions are smaller in ROI_1 than in ROI_2.

Besides, to note that, when SLP gets lower and RH gets larger, the differences of lightning flashes

(polluted minus clean datasets) becomes larger. This suggests that under conductive condition,

aerosols are more likely to participate in cloud process, convection development and thus modulate

lightning activity.

4.5 Relative roles of meteorology and AOD in lightning

The response of lightning to changes in AOD may indicate an aerosol effect on lightning

activity, but can also be the result of meteorology impacting on aerosol loadings and cloud

microphysical process that is closely associated with lightning production. To further explore this

complex process, the correlation of aerosol－lightning, meteorological variables－lightning,

aerosol-meteorological variables were examined before and after the turning point (AOD=0.3)

respectively, results are shown in Fig. 10.

For clean condition (AOD<0.3) in the ROI_1, all meteorological variables and AOD show

good correlations with lightning (Pearson1: ｜R｜>0.5). Considering the interaction between

aerosol and meterology, the correlation coefficients between AOD and six meteorological

variables are calculated. Results show strong and positive correlation between AOD and RH,

CAPE, Div, θ (Pearson2: R>0.6), negative correlation between AOD and SLP, SHEAR (in order

of correlation strength, so as the following). To investigate the relative roles of these variables

(AOD and six meteorological variables), we carry out partial correaltion analyses between

lightning and any influencial factor while constraining all the others, and establish the standardized

402   multiple regression equation, of which the coefficients represent the relative importance of each

403   factor. After the common effects are constrained, partial correlation coefficients are much smaller

404   compared to Pearson correlation coefficients, and the correlation between lightning and SLP, θ,

405   AOD are not significant any more. It's envisioned that lightning doesn't respond much to dust

406   aerosols directly, but dust can affect convection and lightning activities through modulating

407   meterological variables. From these analyses, the top three factors are found to be RH, CAPE, and

408   Div for dust dominant region under relatively clean condition. For clean ROI_2, the analyses show

409   strong positive correlation between lightning and CAPE, AOD, Div (Pearson1:│R│>0.7), strong

410   negative correlation between lightning and SLP (Pearson1: R=-0.94), weak negative correlation

411   between lightning and θ, SHEAR (Pearson1:│R│<0.4). Main interplay exists between AOD and

412   SLP, CAPE (Pearson2:│R│>0.75). The partial correlation coefficients and coefficients of

413   standardized multiple regression equation reveal top three factors: CAPE, AOD, and RH (Partial:

414   R>0.35). Different from RH as the top restraint facotr in dust dominant region, here it plays a

415   smaller role in the humid environment. Besides, AOD becomes more important. In both regions,

416   aerosols correlate well with meterology, which could be the reason for the tight cluster distribution

417   for AOD less than 0.3 in Fig. 9. CAPE measures the amount of moist static energy that is available

418   to drive the convection (Rosenfeld et al., 2008). The high correlation between AOD and CAPE in

419   both regions suggests that aerosol might modulate environment variables and participate in cloud

420   microphysical process. A possible explanation is that more aerosols acting as CCN, lead to

421   narrower cloud droplet size spectrum, delay warm-rain process, allow more liquid water to ascend

422   higher into mixed-phase cloud, thus release more laten heat, produce more unstable atmosphere

423 and larger CAPE which is conductive to convection development. The aerosol invigoration effect

424 may play the key role during this stage (AOD<0.3).

425   Under polluted conditions, CAPE and RH are still of paramount importance for lightning

426 activity (Pearson1: R>0.8; Partial: R>0.35), but the correlation between aerosol and meterology

427 are weakened. This weak connection between aerosol and meterology results in a large dispersion

428 of lighting flashes under polluted conditions in both regions. The most important finding appears

429 to be that the negative correlation of AOD with CAPE (Pearson2: R=-0.51), and RH (Pearson2:

430 R=-0.33) in ROI_1 suggests that increasing dust aerosols may make environment drier, and

431 atmosphere more stable through aerosol radiative effect which leads to the suppression of

432 convection and lightning. While in ROI_2, AOD is negatively correlated with RH (Pearson2: R=-

433 0.24) and θ (Pearson2: R=-0.74) which indicate the similar role of smoke aerosols in making

434 environment drier and surface cooling through radiative effect. But, there's no significant

435 correlation between AOD and CAPE (Pearson2: R=0, p>0.05), which may imply the radiative

436 effect and invigoration effect are comparable under heavy loading codition.

437 ## 5. Conclusions

438   Depending on specific environmental condition, aerosols are able to invigorate or suppress

439 convection induced lightning activity in previous studies, the majority being case based. The

440 controversial conclusions motivate us to study the long-term effects of aerosols and meteorology

441 on lightning activity. Here, meteorology is characterized by six variables: sea level pressure (SLP),

442 potential temperature (θ) at 2 m above ground level, mid-level relative humidity (RH), convective

443   availabe potential energy (CAPE), vertical wind shear (SHEAR), and 200 hPa divergence (Div).

444   The current study investigates the response of lightning activity to meteorology and AOD over

445   dust and smoke dominant regions from a climatological perspective. In particular, 11-year (2003-

446   2013) worth of coincident data are used, including lightning data from LIS/TRMM, AOD from

447   MODIS/Aqua,   and   meteorological   variables   from   ECMWF   ERA-Interim   reanalysis.

448   Climatological features of diurnal and seasonal variations of lightning flashes show the peak in the

449   afternoon and local summer respectively, which suggests a dominant role by thermodynamics,

450   while the differences in lightning under relatively clean and polluted conditions signify the

451   potential influences of aerosols. Specifically, under all stratified meteorological environments,

452   lightning flashes are larger under polluted conditions than under clean condition. And the

453   differences of lightning flashes in ROI_2 are larger than in ROI_1. Besides, lightning flashes

454   increased much more when SLP gets lower and RH gets larger.

455   Despite complex and diverse climatic conditions, the response of lightning to dust and smoke

456   aerosols show in a boomerang shape with an optimum value of AOD around 0.3. We performed

457   correlation analysis and standardized multiple regression analysis in attempt to constrain the

458   effects of meteorology, and quantify the relative roles of these factors in modulating lightning.

459   Under relative clean conditions, standardized multiple regression coefficients of meteorology and

460   AOD on lightning in both regions exhibit $R_M^2 \geq 0.92$, with RH and CAPE being the top two

461   determinant factors. The contribution of RH is comparable with that of CAPE in dust dominant

462   region, and less in smoke aerosols dominant region. The narrow distribution and high correlation

463   between aerosol and meteorology imply that the impact of AOD on lighting activities is likely to

464   be exerted through microphysical effect which modulate meteorological variables. Beyond the

465   optimum value, lightning shows more dispersed distribution and has much weaker dependence on

466   AOD, which may be the consequence of competition between aerosol microphysical effect and

467   radiative effect. Under smoky conditions, R^2_M for the standardized multiple regression equation

468   diminishes to 0.77 with a strong negative correlation (r=-0.74) with θ, and weak negative

469   correlation with mid-level RH and no correlation with CAPE. Note that aerosol cools surface and

470   warms mid-level atmosphere through radiative effect, which may be less (for AOD<0.3), more

471   (AOD>0.3) or equal (AOD=0.3) to the aerosol microphysical effect. Under dusty condition, the

472   standardized equation has a higher R^2_M (0.83), aerosol radiative effect plays a dominant role,

473   possibly leading to stable atmosphere, and suppression of convection and lighting. Lightning

474   responds to AOD in different ways between ROI_1 and ROI_2 mainly because of the different

475   humidity conditions. Totally, for dust dominant region, moisture is the maximum constraint, high

476   CAPE, high RH and moderate aerosol help intensify lightning activity. For smoke dominant region,

477   large values of CAPE, RH and AOD (up to 0.3) fuel lightning. However, the influences of state

478   variables or transient variables (SHEAR, Div) are largely filtered out from the climatological

479   perspective. Until now, we cannot totally filter out, but constrain the confounding effect of

480   meteorological variable on lightning based on observations alone. More insightful analyses are

481   warranted in the future based on a combination of state-of-the-art observations and convection-

482   revolved model simulation.

483

484

485   **Acknowledgements**

486   We gratefully acknowledge GES DISC, NASA DAAC and ECMWF for providing aerosol

487   information, lightning flashes, and meteorological data via public access. MODIS AOD is

488   downloaded from https://ladsweb.modaps.eosdis.nasa.gov/search/. MERRAero are from

489   https://disc.sci.gsfc.nasa.gov/MERRA/; lightning data from https://ghrc.nsstc.nasa.gov/hydro/, the

490   ERA-Interim meteorological data from: http://apps.ecmwf.int/datasets/data/interim-full-moda/.

491   This work was supported by the National Natural Science Foundation of China under grants

492   91544217 and 41771399, Ministry of Science and Technology under grants 2017YFC1501702 and

493   2017YFC1501401, and the Chinese Academy of Meteorological Sciences (2017Z005).

494

References

495 **References**

496 Altaratz, O., Koren, I., Yair, Y., and Price, C.: Lightning response to smoke from Amazonian fires,

497   Geophys. Res. Lett., 37, L07801, https//doi.org/ 10.1029/2010GL042679, 2010.

498 Andreae, M. O.: Biomass burning: its history, use, and distribution and its impact, in: Global

499   Biomass Burning: Atmospheric, Climatic, and Biospheric Implications, MIT Press,

500   Cambridge, MA, 3–21, 1991.

501 Bell, T. L., Rosenfeld, D., Kim, K. M., Yoo, J. M., Lee, M. I., and Hahnenberger, M.: Midweek

502   increase in US summer rain and storm heights suggests air pollution invigorates rainstorms,

503   J. Geophys. Res. - Atmos., 113(D2), https://doi.org/10.1029/2007JD008623, 2008.

504 Bell, T. L., Rosenfeld, D., and Kim, K. M.: Weekly cycle of lightning: evidence of storm

505   invigoration by pollution, Geophys. Res. Lett., 36(23), https://doi.org/10.1029/2009GL040915,

506   2009.

507 Betz, H. D., Schumann, U., and Laroche, P.: Lightning: Principles, Instruments and Applications:

508   Review of Modern Lightning Research, Springer Science & Business Media, 2008.

509 Boccippio, D. J.: Lightning scaling relations revisited, J. Atmos. Sci., 59(6), 1086–1104,

510   https://doi.org/10.1175/1520-0469(2002)059<1086:LSRR>2.0.CO;2, 2002.

511 Boccippio, D. J., Goodman, S. J., and Heckman, S.: Regional differences in tropical lightning

512   distributions, J. Appl. Meteorol., 39(12), 2231–2248, https://doi.org/10.1175/1520-

513   0450(2001)040<2231:RDITLD>2.0.CO;2, 2000.

514 Boucher, O., Randall, D., Artaxo, P., Bretherton, C., Feingold, G., Forster, P., Kerminen, V.-M.,

515   Kondo, Y., Liao, H., Lohmann, U., Rasch, P., Satheesh, S.K., Sherwood, S., Stevens, B., and

516   Zhang, X.Y.: Clouds and Aerosols. In: Climate Change 2013: The Physical Science Basis.

517   Contribution of Working Group I to the Fifth Assessment Report of the Intergovernmental Panel

518   on Climate Change [Stocker, T.F., D. Qin, G.-K. Plattner, M. Tignor, S.K. Allen, J. Boschung,

519   A. Nauels, Y. Xia, V. Bex and P.M. Midgley (eds.)]. Cambridge University Press, Cambridge,

520   United Kingdom and New York, NY, USA., 2013.

521   Burpee, R. W.: The origin and structure of easterly waves in the lower troposphere of North Africa,

522   J. Atmos. Sci., 29(1), 77–90, https://doi.org/10.1175/1520-0469(1972)029<0077:

523   TOASOE>2.0.CO;2, 1972.

524   Cecil, D. J.: LIS/OTD 2.5 Degree Low Resolution Diurnal Climatology (LRDC) [indicate subset

525   used]. Dataset available online from the NASA Global Hydrology Center DAAC, Huntsville,

526   Alabama, U.S.A, doi: http://dx.doi.org/10.5067/LIS/LIS-OTD/DATA307, 2001.

527   Cecil, D. J.: LIS/OTD 2.5 Degree Low Resolution Monthly Climatology Time Series (LRMTS)

528   [indicate subset used]. Dataset available online from the NASA Global Hydrology Center

529   DAAC, Huntsville, Alabama, U.S.A, doi: http://dx.doi.org/10.5067/LIS/LIS-OTD/DATA309,

530   2006.

531   Cecil, D. J., Buechler, D. E., and Blakeslee, R. J.: Gridded lightning climatology from TRMM-

532   LIS and OTD: dataset description, Atmos. Res., 135, 404–414,

533   https://doi.org/10.1016/j.atmosres.2012.06.028, 2014.

534   Christian, H. J., Blakeslee, R. J., Boccippio, D. J., Boeck, W. L., Buechler, D. E., Driscoll, K. T.,

535   Goodman, S. J., Hall, J. M., Koshak, W. J., and Mach, D. M.: Global frequency and

536   distribution of lightning as observed from space by the Optical Transient Detector, J. Geophys.

537 Res. - Atmos., 108(D1), https://doi.org/10.1029/2002JD002347, 2003.

538 Coniglio, M. C., Stensrud, D. J., and Wicker, L. J.: Effects of upper-level shear on the structure

539 and maintenance of strong quasi-linear mesoscale convective systems, J. Atmos. Sci., 63(4),

540 1231–1252, https://doi.org/10.1175/JAS3681.1, 2006.

541 da Silva, A. M., Randles, C. A., Buchard, V., Darmenov, A., Colarco, P. R., and Govindaraju, R,:

542 File Specification for the MERRA Aerosol Reanalysis (MERRAero). GMAO Office Note No.

543 7 (available from http://gmao.gsfc.nasa.gov/pubs/office_notes), 2015

544 Dee, D. P., Uppala, S., Simmons, A., Berrisford, P., Poli, P., Kobayashi, S., Andrae, U., Balmaseda,

545 M., Balsamo, G., and Bauer, P.: The ERA-Interim reanalysis: configuration and performance

546 of the data assimilation system, Q. J. Roy. Meteorol. Soc., 137(656), 553–597,

547 https://doi.org/10.1002/qj.828, 2011.

548 Fan, J., Zhang, R., Li, G., and Tao, W. K.: Effects of aerosols and relative humidity on cumulus

549 clouds, J. Geophys. Res. - Atmos., 112(D14), https://doi.org/10.1029/2006JD008136, 2007.

550 Fan, J., Leung, L. R., Rosenfeld, D., Chen, Q., Li, Z., Zhang, J., and Yan, H.: Microphysical effects

551 determine macrophysical response for aerosol impacts on deep convective clouds, P. Natl.

552 Acad. Sci. USA, 110(48), E4581-E4590, https://doi.org/10.1073/pnas.1316830110, 2013.

553 Fan, J., Yuan, T., Comstock, J. M., Ghan, S., Khain, A., Leung, L. R., Li, Z., Martins, V. J., and

554 Ovchinnikov, M.: Dominant role by vertical wind shear in regulating aerosol effects on deep

555 convective clouds, J. Geophys. Res. - Atmos., 114(D22), https://doi.org/

556 10.1029/2009JD012352, 2009.

557 Fan J, Wang, Y., Rosenfeld, D., and Liu, X.: Review of Aerosol-Cloud Interactions: Mechanisms,

558   Significance and Challenges. Journal of the Atmospheric Sciences, 73(11):4221-

559   4252., doi:10.1175/JAS-D-16-0037.1, 2016.

560   Fan, J., Rosenfeld, D., Ding, Y., Leung, L. R., and Li, Z.: Potential aerosol indirect effects on

561   atmospheric circulation and radiative forcing through deep convection, Geophys. Res. Lett.,

562   39(9), https://doi.org/10.1029/2012GL051851, 2012.

563   Farias, W., Pinto Jr., O., Pinto, I., and Naccarato, K.: The influence of urban effect on lightning

564   activity: evidence   of   weekly   cycle,   Atmos.   Res.,   135,   370–373,

565   https://doi.org/10.1016/j.atmosres.2012.09.007, 2014.

566   Goudie, A., and Middleton, N.: Saharan dust storms: nature and consequences, Earth-Sci. Rev.,

567   56(1–4), 179–204, https://doi.org/10.1016/S0012-8252(01)00067-8, 2001.

568   Guo, J., Deng, M., Lee, S. S., Wang, F., Li, Z., Zhai, P., Liu, H., Lv, W., Yao, W., and Li, X.:

569   Delaying precipitation and lightning by air pollution over the Pearl River Delta. Part I:

570   Observational   analyses,   J.   Geophys.   Res.   -   Atmos.,   121(11),   6472–6488,

571   https://doi.org/10.1002/2015JD023257, 2016.

572   Hintze, J. L., and Nelson, R. D.: Violin plots: a box plot-density trace synergism, The American

573   Statistician, 52(2), 181–184, https://doi.org/10.1080/00031305.1998.10480559, 1998.

574   Homeyer, C. R., Schumacher, C., and Hopper Jr., L. J.: Assessing the applicability of the tropical

575   convective–stratiform paradigm in the extratropics using radar divergence profiles, J. Climate,

576   27(17), 6673–6686, https://doi.org/10.1175/JCLI-D-13-00561.1, 2014.

577   Hubanks, P., Platnick, S., King, M., and Ridgway, B.: MODIS Atmosphere L3 gridded product

578   algorithm theoretical basis document (atbd) & users guide, ATBD reference number ATBD-

579   MOD-30, NASA, 125, 2015.

580   Ichoku, C., Ellison, L. T., Willmot, K. E., Matsui, T., Dezfuli, A. K., Gatebe, C. K., Wang, J.,

581   Wilcox, E. M., Lee, J., and Adegoke, J.: Biomass burning, land-cover change, and the

582   hydrological cycle in Northern sub-Saharan Africa, Environ. Res. Lett., 11(9),

583   https://doi.org/10.1088/1748-9326/11/9/095005, 2016.

584   Igel, M. R., and Heever, S. C.: The relative influence of environmental characteristics on tropical

585   deep convective morphology as observed by CloudSat, J. Geophys. Res. - Atmos., 120(9),

586   4304–4322, https://doi.org/10.1002/2014JD022690, 2015.

587   Kaufman, Y. J., Tanre, D., Holben, B., Mattoo, S., Remer, L., Eck, T., Vaughan, J., and Chatenet,

588   B.: Aerosol radiative impact on spectral solar flux at the surface, derived from principal-plane

589   sky measurements, J. Atmos. Sci., 59(3), 635–646, https://doi.org/10.1175/1520-

590   0469(2002)059<0635:ARIOSS>2.0.CO;2, 2002.

591   Khain, A. P.: Notes on state-of-art investigation of aerosol effects on precipitation: A critical review,

592   Environ. Res. Lett., 4, 015004, doi:10.1088/1748-9326/4/1/015004, 2009.

593   Khain, A., and Lynn, B.: Simulation of a supercell storm in clean and dirty atmosphere using

594   weather research and forecast model with spectral bin microphysics, J. Geophys. Res. -

595   Atmos., 114(D19), https://doi.org/10.1029/2009JD011827, 2009.

596   Khain, A., Pokrovsky, A., Pinsky, M., Seifert, A., and Phillips, V.: Simulation of effects of

597   atmospheric aerosols on deep turbulent convective clouds using a spectral microphysics

598   mixed-phase cumulus cloud model. Part I: Model description and possible applications, J.

599   Atmos. Sci., 61(24), 2963–2982, https://doi.org/10.1175/JAS-3350.1, 2004.

Khain, A., Rosenfeld, D., and Pokrovsky, A.: Aerosol impact on the dynamics and microphysics of deep convective clouds, Q. J. Roy. Meteorol. Soc., 131(611), 2639–2663, https://doi.org/10.1256/qj.04.62, 2005.

Khain, A., BenMoshe, N., and Pokrovsky, A.: Factors determining the impact of aerosols on surface precipitation from clouds: an attempt at classification, J. Atmos. Sci., 65(6), 1721–1748, https://doi.org/10.1175/2007JAS2515.1, 2008.

Knaff, J. A.: Implications of summertime sea level pressure anomalies in the tropical Atlantic region, J. Climate, 10(4), 789–804, https://doi.org/10.1175/1520-0442(1997)010<0789: IOSSLP>2.0.CO;2, 1997.

Koren, I., Kaufman, Y. J., Remer, L. A., and J. V. Martins, J. V.: Measurement of the effect of Amazon smoke on inhibition of cloud formation, Science, 303(5662), 1342–1345, https://doi.org/10.1126/science.1089424, 2004.

Koren, I., Martins, J. V., Remer, L. A., and Afargan, H.: Smoke invigoration versus inhibition of clouds over the Amazon, Science, 321(5891), 946–949, https://doi.org/10.1126/science.1159185, 2008.

Lee, S. S., Guo, J., and Li, Z.: Delaying precipitation by air pollution over the Pearl River Delta: 2. Model simulations, J. Geophys. Res. - Atmos., 121(19), https://doi.org/10.1002/2015JD024362, 2016.

Lemaître, C., Flamant, C., Cuesta, J., Raut, J.-C., Chazette, P., Formenti, P., and Pelon, J.: Radiative heating rates profiles associated with a springtime case of Bodélé and Sudan dust transport over West Africa, Atmos. Chem. Phys., 10(17), 8131–8150, https://doi.org/10.5194/acp-10-

621   8131-2010, 2010.

622   Levy, R., Mattoo, S., Munchak, L., Remer, L., Sayer, A., Patadia, F., and Hsu, N.: The Collection

623   6 MODIS aerosol products over land and ocean, Atmos. Measurement Tech., 6(11), 2989–

624   3034, https://doi.org/10.5194/amt-6-2989-2013, 2013.

625   Li, Z., Lau, W. M., Ramanathan, V., Wu, G., Ding, Y., Manoj, M., Liu, J., Qian, Y., Li, J., and Zhou,

626   T.: Aerosol and monsoon climate interactions over Asia, Rev. Geophys., 54(4), 866–929,

627   https://doi.org/10.1002/2015RG000500, 2016.

628   Li Z., Guo, J., Ding, A., Liao, H., Liu, J., Sun, Y., Wang, T., Xue, H., Zhang, H., and Zhu, B.:

629   Aerosol and boundary-layer interactions and impact on air quality. National Science Review, 4

630   (6), 810–833. doi: 10.1093/nsr/nwx117, 2017a.

631   Li, Z., Rosenfeld, D., and Fan, J.: Aerosols and their impact on radiation, clouds, precipitation, and

632   severe   weather   events,   Oxford   Research   Encyclopedias,

633   https://doi.org/10.1093/acrefore/9780199389414.013.126, 2017b.

634   Lucas, C., Zipser, E. J., and Lemone, M. A.: Vertical velocity in oceanic convection off tropical

635   Australia,   J.   Atmos.   Sci.,   51(21),   3183–3193,   https://doi.org/10.1175/1520-

636   0469(1994)051<3183:VVIOCO>2.0.CO;2, 1994.

637   Mapes, B., and Houze Jr., R. A.: An integrated view of the 1987 Australin monsoon and its

638   mesoscale convective systems. II: Vertical structure, Q. J. Roy. Meteorol. Soc., 119(512),

639   733–754, https://doi.org/10.1002/qj.49711951207, 1993.

640   Mapes, B. E., and Houze Jr., R. A.: Diabatic divergence profiles in western Pacific mesoscale

641   convective systems, J. Atmos. Sci., 52(10), 1807–1828, https://doi.org/10.1175/1520-

642   0469(1995)052<1807:DDPIWP>2.0.CO;2, 1995.

643   Markson, R.: Ionospheric potential variation from temperature change over continents, XII

644   International Conference on Atmospheric Electricity, Versailles, France, 2003.

645   Menon, S., Hansen, J., Nazarenko, L., and Luo, Y.: Climate effects of black carbon aerosols in

646   China and India, Science, 297(2250), 2002.

647   Mitovski, T., Folkins, I., Von Salzen, K., and Sigmond, M.: Temperature, relative humidity, and

648   divergence response to high rainfall events in the tropics: observations and models, J. Climate,

649   23(13), 3613–3625, https://doi.org/10.1175/2010JCLI3436.1, 2010.

650   Nesbitt, S. W., and Zipser, E. J.: The diurnal cycle of rainfall and convective intensity according

651   to three years of TRMM measurements, J. Climate, 16(10), 1456–1475,

652   https://doi.org/10.1175/1520-0442-16.10.1456, 2003.

653   Orville, R. E., Huffines, G., Nielsen-Gammon, J., Zhang, R., Ely, B., Steiger, S., Phillips, S., Allen,

654   S., and Read, W.: Enhancement of cloud-to-ground lightning over Houston, Texas, Geophys.

655   Res. Lett., 28(13), 2597–2600, https://doi.org/10.1029/2001GL012990, 2001.

656   Price, C.: Global surface temperatures and the atmospheric electrical circuit, Geophys. Res. Lett.,

657   20(13), 1363–1366, https://doi.org/10.1029/93GL01774, 1993.

658   Prospero, J. M., Ginoux, P., Torres, O., Nicholson, S. E., and Gill, T. E.: Environmental

659   characterization of global sources of atmospheric soil dust derived from the Nimbus 7 TOMS

660   absorbing aerosol product, Rev. Geophys., 40(1), https://doi.org/10.1029/2000RG000095,

661   2002.

662   Richardson, Y. P., Droegemeier, K. K., and Davies-Jones, R. P.: The influence of horizontal

663   environmental variability on numerically simulated convective storms. Part I: Variations in

664   vertical shear, Mon. Weather Rev., 135(10), 3429–3455, https://doi.org/10.1175/MWR3463.1,

665   2007.

666   Riemann-Campe, K., Fraedrich, K., and Lunkeit, F.: Global climatology of convective available

667   potential energy (CAPE) and convective inhibition (CIN) in ERA-40 reanalysis, Atmos. Res.,

668   93(1-3), 534–545, https://doi.org/10.1016/j.atmosres.2008.09.037, 2009.

669   Roberts, G., Wooster, M., and Lagoudakis, E.: Annual and diurnal African biomass burning

670   temporal dynamics, Biogeosci., 6(5), https://doi.org/10.5194/bg-6-849-2009, 2009.

671   Rosenfeld, D., and Lensky, I. M.: Satellite–based insights into precipitation formation processes

672   in continental and maritime convective clouds, Bull. Amer. Meteorol. Soc., 79(11), 2457–

673   2476, https://doi.org/10.1175/1520-0477(1998)079<2457:SBIIPF>2.0.CO;2, 1998.

674   Rosenfeld, D., Rudich, Y., and Lahav, R.: Desert dust suppressing precipitation: a possible

675   desertification   feedback   loop,   P.   Natl.   Acad.   Sci.   USA,   98(11),   5975–5980,

676   https://doi.org/10.1073/pnas.101122798, 2001.

677   Rosenfeld, D., Lohmann, U., Raga, G. B., O'Dowd, C. D., Kulmala, M., Fuzzi, S., Reissell, A.,

678   and Andreae, M. O.: Flood or drought: How do aerosols affect precipitation?, Science,

679   321(5894), 1309–1313, https://doi.org/ 10.1126/science.1160606, 2008.

680   Rotunno, R., Klemp, J. B., and Weisman, M. L.: A theory for strong, long-lived squall lines, J.

681   Atmos.   Sci.,   45(3),   463–485,   https://doi.org/10.1175/1520-

682   0469(2004)061<0361:ATFSLS>2.0.CO;2, 1998.

683   Shao, Y.: Physics and Modelling of Wind Erosion, Springer Science & Business Media, 2008.

684 Stolz, D. C., Rutledge, S. A., and Pierce, J. R.: Simultaneous influences of thermodynamics and

685   aerosols on deep convection and lightning in the tropics, J. Geophys. Res. - Atmos., 120(12),

686   6207–6231, https://doi.org/10.1002/2014JD023033, 2015.

687 Stolz, D. C., Rutledge, S. A., Pierce, J. R., and Heever , S. C.: A global lightning parameterization

688   based on statistical relationships among environmental factors, aerosols, and convective

689   clouds in the TRMM climatology, J. Geophys. Res. - Atmos., 122, 7461–7492, https://doi.org/

690   10.1002/2016JD026220, 2017.

691 Tao, W. K., Li, X., Khain, A., Matsui, T., Lang, S., and Simpson, J.: Role of atmospheric aerosol

692   concentration on deep convective precipitation: cloud-resolving model simulations, J.

693   Geophys. Res. - Atmos., 112(D24), https://doi.org/10.1029/2007JD008728, 2007.

694 Tao, W. K., Chen, J. P., Li, Z. Q., Wang, C., and Zhang, C. D.: Impact of aerosols on convective

695   clouds and precipitation. Reviews of Geophysics, 50 (RG2001), doi: 10.1029/2011rg000369,

696   2012.

697 Thornton, J. A., Virts, K. S., Holzworth, R. H., and Mitchell, T. P.: Lightning enhancement over

698   major   oceanic   shipping   lanes,   Geophys.   Res.   Lett.,   44(17),   9102–9111,

699   https://doi.org/10.1002/2017GL074982, 2017.

700 van der Werf, G. R., Randerson, J. T., Collatz, G. J., and Giglio, L.: Carbon emissions from fires

701   in   tropical   and   subtropical   ecosystems,   Global   Change   Biology,   9(4),   547–562,

702   https://doi.org/10.1046/j.1365-2486.2003.00604.x, 2003.

703 van der Werf, G. R., Randerson, J. T., Giglio, L., Collatz, G. J., Kasibhatla, P. S., and Arellano Jr.,

704   A. F.: Interannual variability in global biomass burning emissions from 1997 to 2004, Atmos.

705   Chem. Phys., 6(11), 3423–3441,   https://doi.org/10.5194/acp-6-3423-2006, 2006.

706 Waliser, D. E., and Gautier, C.: A satellite-derived climatology of the ITCZ, J. Climate, 6(11),

707   2162–2174, https://doi.org/10.1175/1520-0442(1993)006<2162:ASDCOT>2.0.CO;2, 1993.

708 Wall, C., Zipser, E., and Liu, C.: An investigation of the aerosol indirect effect on convective

709   intensity   using   satellite   observations,   J.   Atmos.   Sci.,   71(1),   430–447,

710   https://doi.org/10.1175/JAS-D-13-0158.1, 2014.

711 Wang, F., Guo, J., Zhang, J., Huang, J., Min, M., Chen, T., Liu, H., Deng, M., and Li,X.: Multi-

712   sensor quantification of aerosol-induced variability in warm cloud properties over eastern China,

713   Atmospheric Environment, 113, 1-9, 2015.

714 Weisman, M. L., and Rotunno, R.: "A theory for strong long-lived squall lines" revisited, J. Atmos.

715   Sci., 61(4), 361–382, https://doi.org/10.1175/1520-0469(2004)061<0361:ATFSLS>2.0.CO;2,

716   2004.

717 Westcott, N. E.: Summertime cloud-to-ground lightning activity around major Midwestern urban

718   areas, J. Appl. Meteorol., 34(7), 1633–1642, https://doi.org/10.1175/1520-0450-34.7.1633,

719   1995.

720 Williams, E.: Global circuit response to temperature on distinct time scales: a status report,

721   Atmospheric and Ionospheric Phenomena Associated with Earthquakes, 939–949, 1999.

722 Williams, E.: Lightning   and   climate: a   review,   Atmos.   Res.,   76(1-4),   272–287,

723   https://doi.org/10.1016/j.atmosres.2004.11.014, 2005.

724 Williams, E., and Stanfill, S.: The physical origin of the land–ocean contrast in lightning activity,

725   Comptes   Rendus   Physique,   3(10),   1277–1292,   https://doi.org/10.1016/S1631-

726   0705(02)01407-X, 2002.

727   Williams, E., Chan, T., and Boccippio, D.: Islands as miniature continents: another look at the

728   land-ocean   lightning   contrast,   J.   Geophys.   Res.   -   Atmos.,   109(D16),

729   https://doi.org/10.1029/2003JD003833, 2004.

730   Williams, E., Mushtak, V., Rosenfeld, D., Goodman, S. and Boccippio, D.: Thermodynamic

731   conditions favorable to superlative thunderstorm updraft, mixed phase microphysics and

732   lightning   flash   rate,   Atmos.   Res.,   76(1-4),   288–306,

733   https://doi.org/10.1016/j.atmosres.2004.11.009, 2005.

734   Williams, E. R.: The Schumann resonance: a global tropical thermometer, Science, 256(5060),

735   1184–1187, https://doi.org/10.1126/science.256.5060.1184, 1992.

736   Williams, E. R.: Global circuit response to seasonal variations in global surface air temperature,

737   Mon.   Weather   Rev.,   122(8),   1917–1929,   https://doi.org/10.1175/1520-

738   0493(1994)122<1917:GCRTSV>2.0.CO;2, 1994.

739   Ye, B., Del Genio, A. D., and Lo, K. K.: CAPE variations in the current climate and in a climate

740   change, J. Climate, 11(8), 1997–2015, https://doi.org/10.1175/1520-0442-11.8.1997, 1998.

741   Yuan, T., Remer, L. A., Pickering, K. E., and Yu, H.: Observational evidence of aerosol

742   enhancement of lightning activity and convective invigoration, Geophys. Res. Lett., 38(4),

743   https://doi.org/10.1029/2010GL046052, 2011.

744   Zhao, C., Tie, X., and Lin, Y.: A possible positive feedback of reduction of precipitation and

745   increase   in   aerosols   over   eastern   central   China,   Geophys.   Res.   Lett.,   33(11),

746   https://doi.org/10.1029/2006GL025959, 2006.

747   Zipser, E. J., and Lutz, K. R.: The vertical profile of radar reflectivity of convective cells: a strong

748   indicator of storm intensity and lightning probability? Mon. Weather Rev., 122(8), 1751–1759,

749   https://doi.org/10.1175/1520-0493(1994)122<1751:TVPORR>2.0.CO;2, 1994.

750

751

752
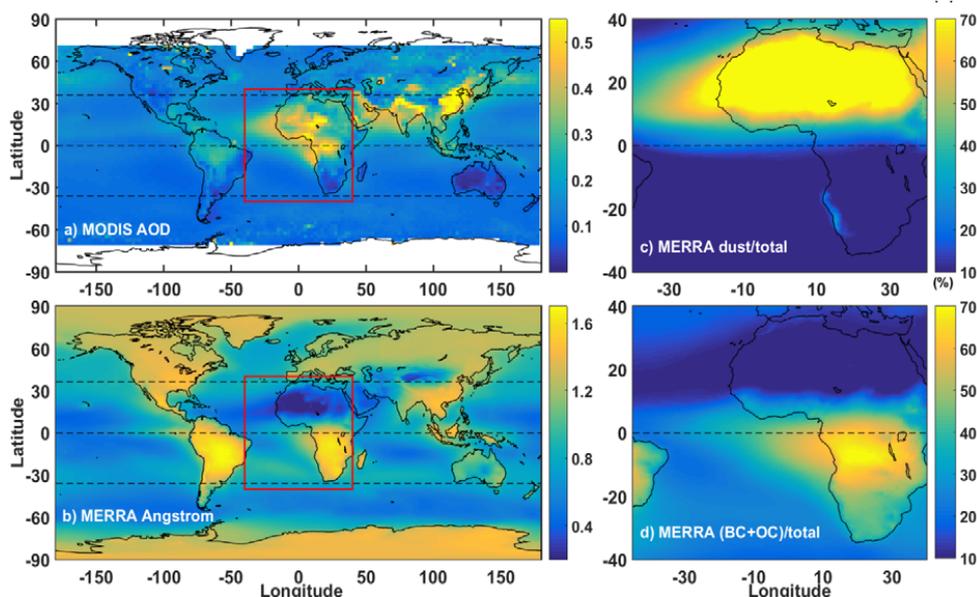
Figure 1. Global spatial distribution maps of (a) AOD (550 nm) as derived from MODIS at a spatial resolution of 1°×1°, and (b) Total aerosol angstrom parameter (470-870 nm) from MERRA dataset on a 0.625°×0.5° grid for the period 2003-2013. Also shown is the distribution of the ratio of dust AOD to total AOD over the region of interest outlined in red box (in panel a), and panel d is same as panel c, but for the ratio of (BC+OC) AOD to total AOD. Dust, black carbon, organic carbon and total extinction AOD used here are all derived from MERRAero dataset (da Silva et al., 2015).
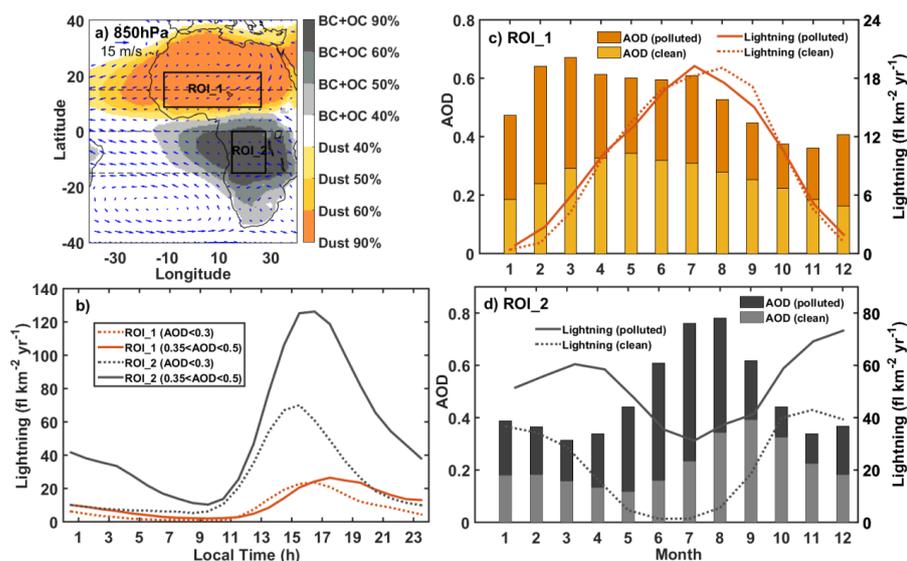
Figure 2. (a) The distribution of 850 hPa mean wind field from ERA-Interim re-analysis with a spatial resolution of 1°×1° showing the prevailing wind direction over Africa and the   neighbouring ocean over the region of interest (ROI) defined in Fig. 1. ROI_1 and ROI_2 (highlighted in black rectangles) are chosen with the ratio of dust or (BC+OC) extinction AOD to total extinction AOD being greater than 50% averaged over the period from 2003 to 2013, which enable us to better understand the potential effect of dust or smoke aerosols on lightning, respectively. Also shown are the diurnal cycle (b) and monthly variation (c, d) of AOD and lightning flashes as caculated under relatively clean and polluted (dusty/smoky) conditions in dust dominant region (ROI_1) and smoke dominant region (ROI_2), respectively. Unless noted otherwise, AOD used in this study is derived from MODIS, and the lowest (highest) third of AOD is labeled as clean (polluted) condition. Lightning flashes come from the low resolution monthly time series (LRMTS) and the low resolution diurnal climatology (LRDC) products on a 2.5°×2.5° grid (Ceil et al., 2001; 2006; 2014).
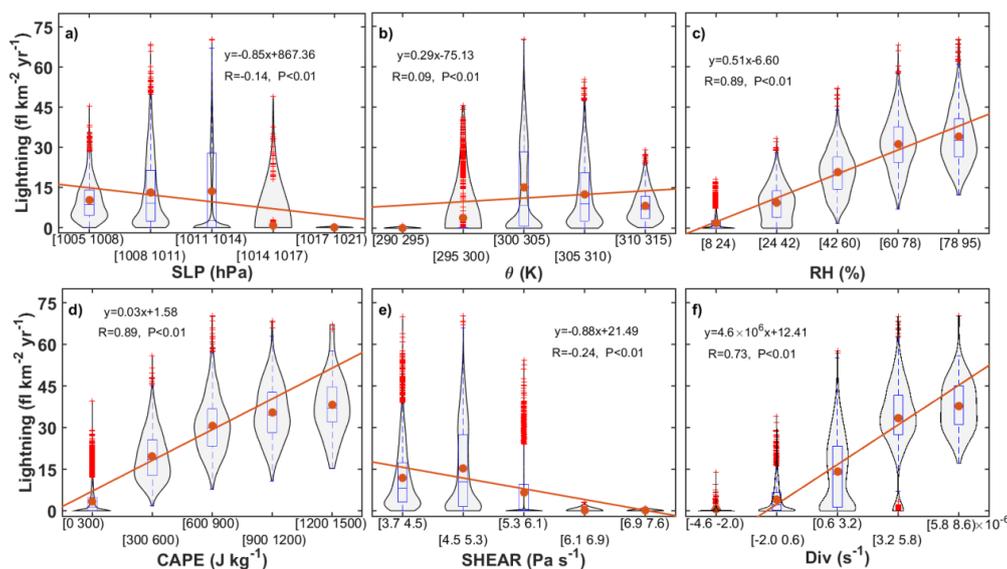
Figure 3. Violin plots of lightning dispersion showing the relationship of lightning with six meteorological variables (SLP, θ, RH, CAPE, SHEAR, Div) in ROI_1. The five bins are equally-spaced. Box plots represent the interquartile range (the distance between the bottom and the top of the box), median (the band inside the box), 95% confidence interval (whiskers above and below the box) of the data, maximum (the end of the whisker above), minimum (the end of the whisker below), mean (orange dot) in each bin. Red '+' represent outliers. On each side of the black line is the kernel estimation to show the distribution shape of the data. The estimate is based on a normal kernel function, and is evaluated at 100 equally spaced points. Wider sections of the violin plot represent a high probability that members of the population will take on the given value; the skinnier sections represent a lower probability. The equations show the linear relationships (orange lines) between lightning and meteorological variables. Also given are Pearson correlation coefficients (R), p values and linear regression lines (in orange).
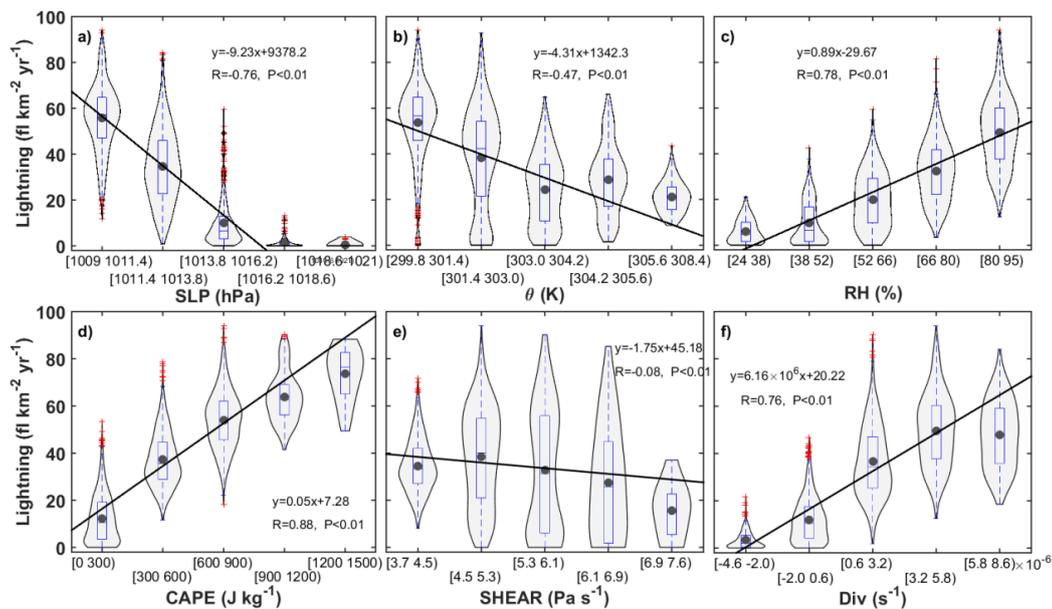
Figure 4. Same as in Fig. 3, but for ROI_2. The mean values are represented by black dots, and the linear regression lines are shown in black.
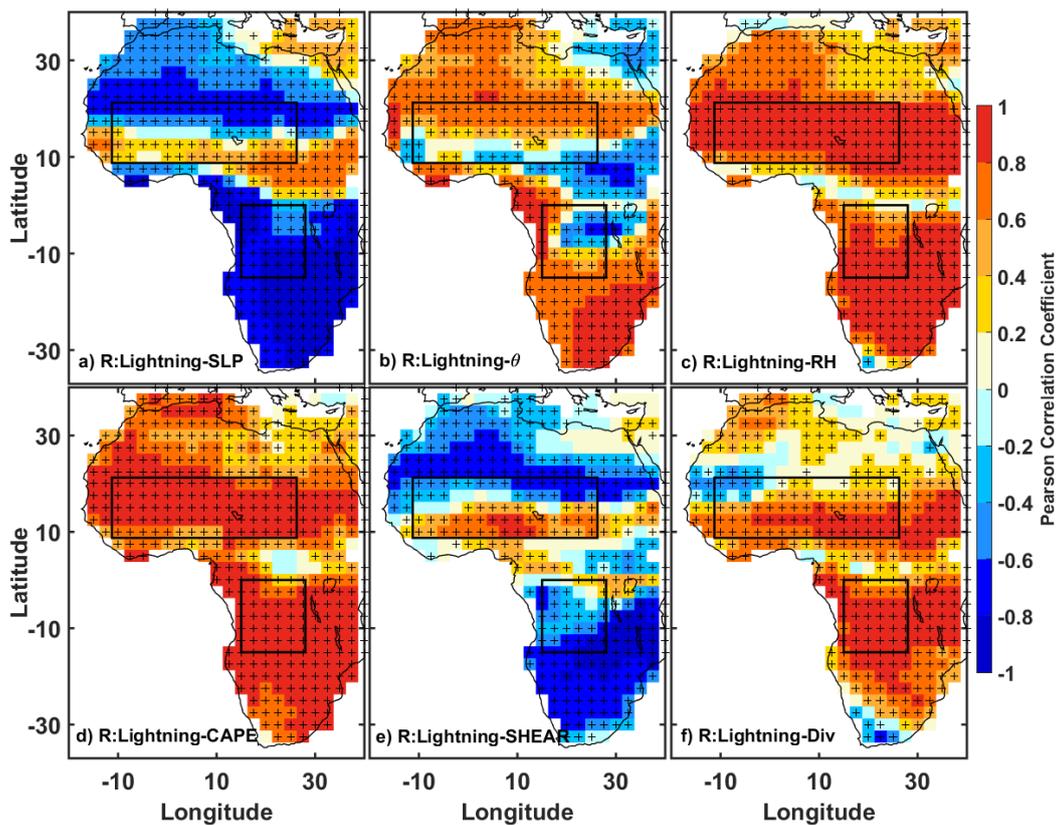
Figure 5. The map of Pearson correlation coefficients between lightning flashes and (a) sea level pressure (SLP), (b) potential temperature (θ), (c) mid-level relative humidity (RH) , (d) mean convective available potential energy (CAPE), (e) vertical wind shear (SHEAR), and (f) 200 hPa divergence (Div) over Africa. ROI_1 and ROI_2 (see Fig. 2. left panel) are outlined with black boxes. '+' denotes thoses grids which pass the significance test of 0.05.
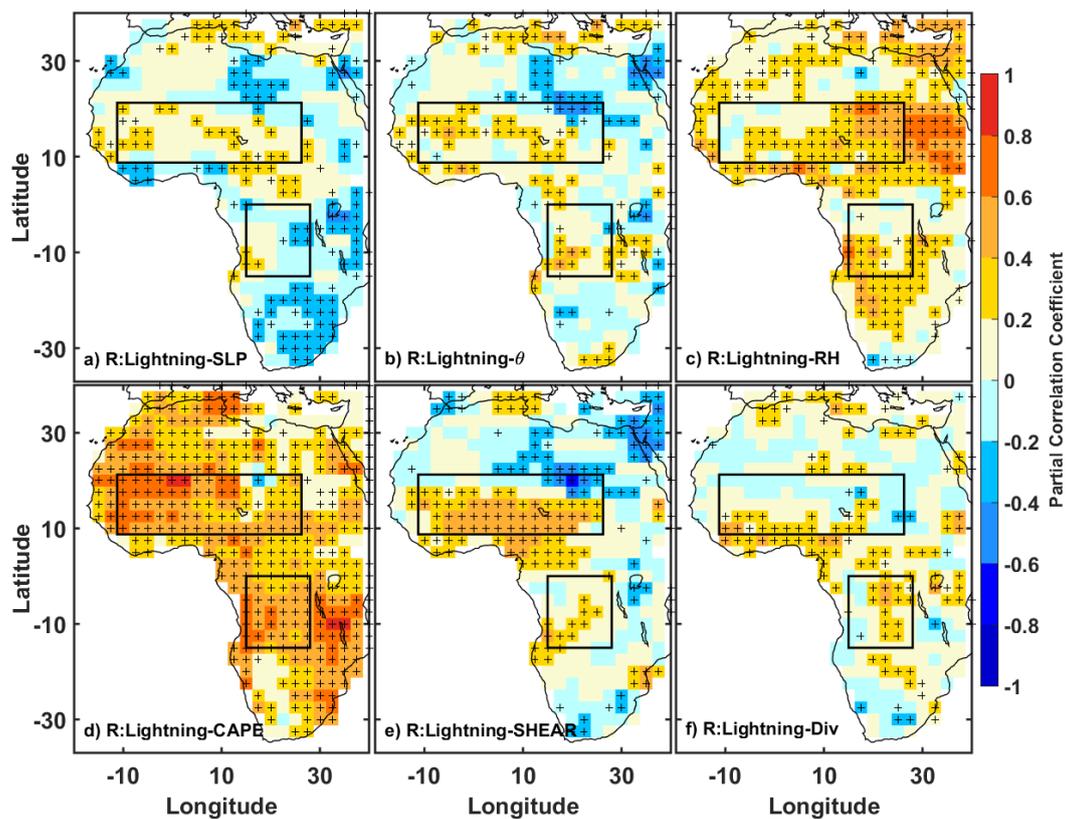
Figure 6. Same as in Fig. 5, but for partial correlation coefficients between lightning flashes and any meteorological variable while controlling AOD and the other five meteorological variables.
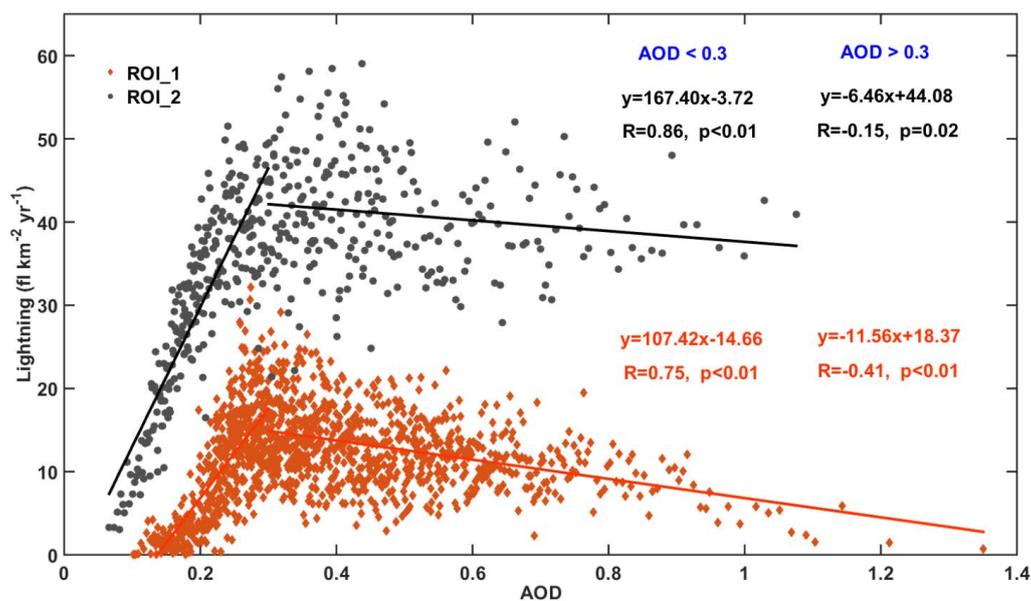
Figure 7. Scatter plot showing the response of lightning to dust or smoke aerosols in a boomerange shape in both ROI_1 and ROI_2. Turning points are around AOD=0.3. Regressions are calculated before and after the turning points in these two regions of interest. Regression equations, correlation coefficients (R), p values, and linear fitting curves are in black (orange) for ROI_1 (ROI_2). All data used here are processed with taking an average of 10 samples after ordering AOD from small to large to reduce the uncertainty caused by large dispersion of data .
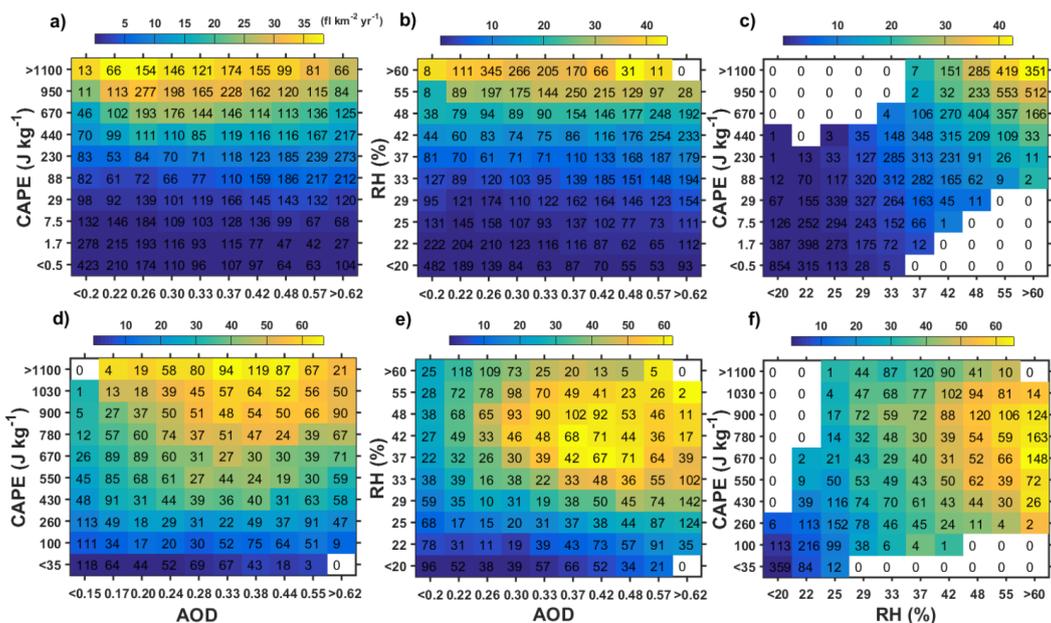
Figure 8. Joint dependence of lightning flashes on CAPE, RH, and AOD in both ROI_1 (a-c) and ROI_2 (d-f), respectively. Bold number in each cell indicate the number of samples in each cell. Colorbar denotes the number of lightning flashes averaged in each cell.
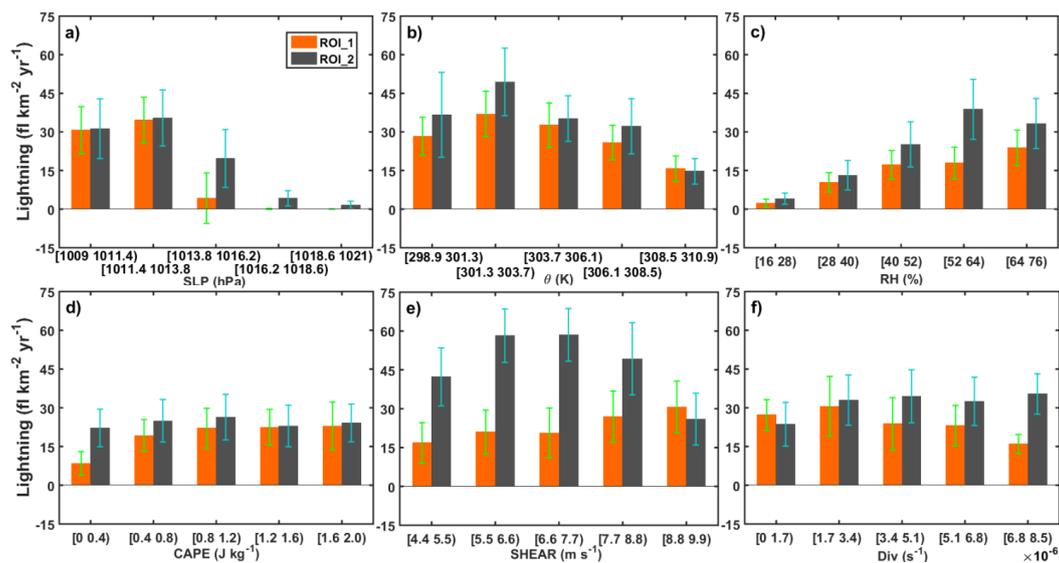
Figure 9. Differences (polluted minus clean subsets of data) of lightning flashes as a function of (a)sea level pressure (SLP), (b) potential temperature (θ), (c) mid-level relative humidity (RH) , (d) convective available potential energy (CAPE), (e) vertical wind shear (SHEAR), (f) 200 hPa divergence (Div) in ROI_1 (in orange) and ROI_2 (in black). Note that, the top third of AOD is labeled as polluted case and the bottom third is labeled as clean case. Vertical error bars represent one standard deviation.
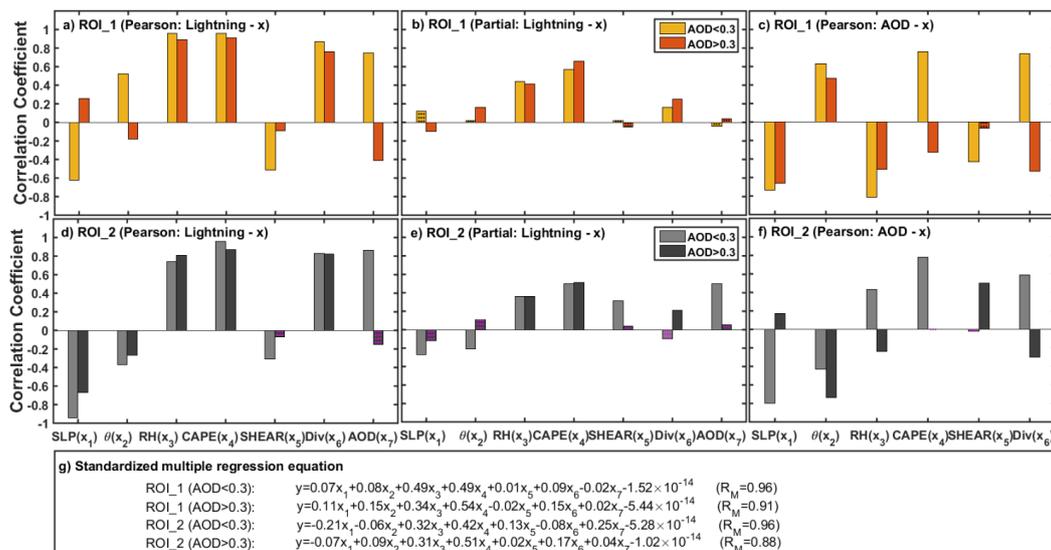
Figure 10. Correlations between AOD and meteorology, and between lightning and meteorology, AOD. (a,d) Pearson correlation coefficients between lightning and six meteorological variables and AOD (Pearson1). (b,e) Partial correlation coefficients between lightning and any influential factor (AOD or meteorological variable) while controlling the other variables (Partial). (c,f) Pearson correlation coefficients between AOD and any given meteorological variable (Pearson2). Those bars with black dots denote that they fail the statistical significance test at 95% confidence level. Also shown are standardized multiple regression equations of lightning (y) onto six meterological variables (x_1-x_6) and AOD (x_7), and standardized multiple correlation coefficients (R_M). Six meterological variables are SLP (x_1), θ (x_2), RH (x_3), CAPE (x_4), SHEAR (x_5), and Div (x_6).